0.4 MPa at a point 5 mm from the heated surface at 2.7 minutes, then reached 6 MPa at a point 10 mm from the heated surface at 6 minutes. When explosive spalling occurred, vapor pressure had built to 4.5 and 6 MPa at points 5 and 10 mm from the heated surface, respectively.

Figure 10 shows depths of spalling after the heating test. The maximum value was about 60 mm, and the depth at the center part was greater than that at the outer part. The specimens were severely damaged.

Figure 11 shows the relationship between spalling depth and time during the heating test. Spalling began approximately 3 minutes after heating began and ended at 12 minutes at a depth of 50 mm.

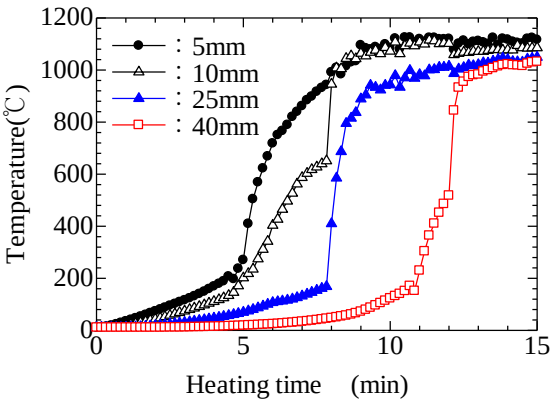

Fig. 7 Temperature and heating time

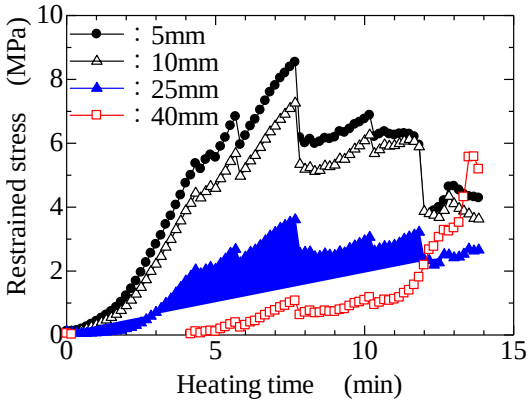

Fig. 8 Thermal stress and heating time

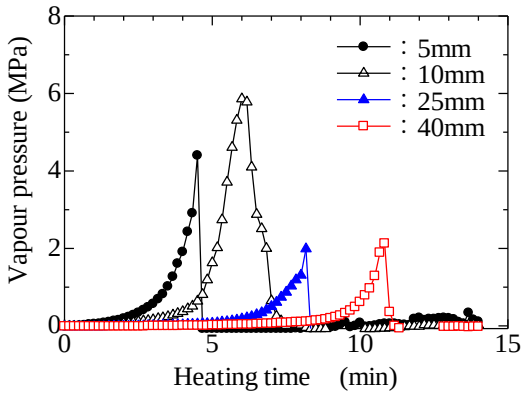

Fig. 9 Vapor pressure and heating time

Fig. 10 Spalling after heating test

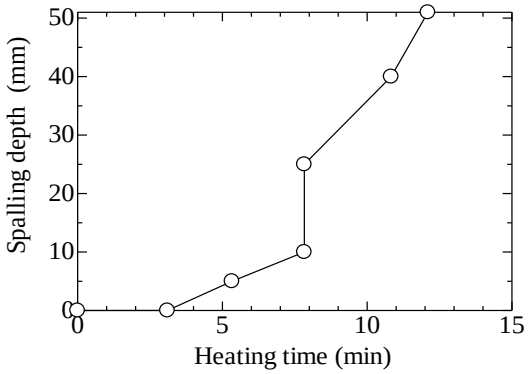

Fig. 11 Spalling depth and heating time

4. NUMERICAL SIMULATION OF FIRE-RELATED SPALLING

4.1 Outline of FEM analysis

Figure 12 shows fire spalling analysis of the specimen containing a restraining ring of radius 150 mm, height 100 mm and thickness 8 mm. An axial symmetry model was used in conjunction with the finite element method. ASTEA-MACS analysis code was used for thermal and stress analysis, and the bottom of the steel ring was insulated. The bottom and open part of the specimen was heated, with a RABT 30 heating curve adopted for the bottom (Fig. 6). The heat transfer coefficient of the bottom part of the concrete was 30 W/m^2°C, and the corresponding figures for the steel ring and the upper part of the concrete were 10 and 12 W/m^2°C, respectively. Figures 13 to 14 show how the thermal conductivity of concrete and steel depend on temperature, Figure 15 shows specific heat and related temperature, and Figures 16 to 20 show the residual compressive strength, elastic modulus and tensile strength and temperature of the concrete and steel ring, respectively.

4.2 Spalling model criteria

The index of the strain failure model I_u as shown in Equation (5) was used in this study. It is assumed that tensile strain failure and concrete spalling occur when *Iu* exceeds the value of 1.0. The apparent Poisson's ratio is 0.2, and the ultimate strain upon tensile failure is 500 μ.

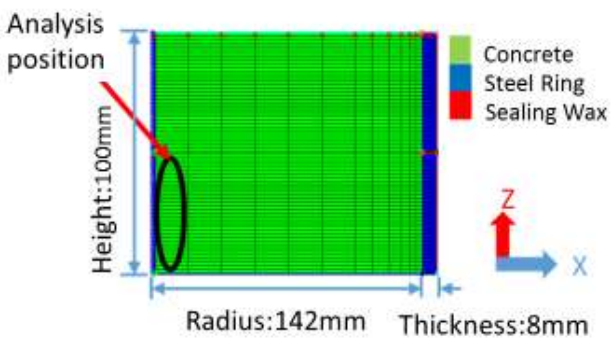

Fig. 12 Axial symmetry model

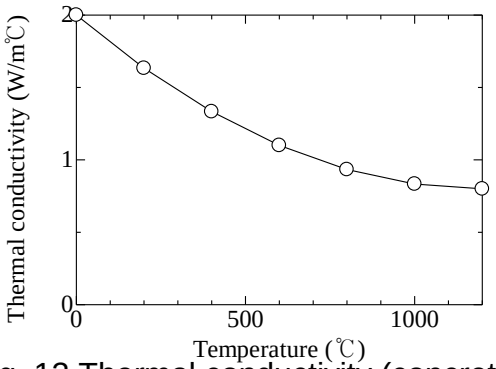

Fig. 13 Thermal conductivity (concrete)

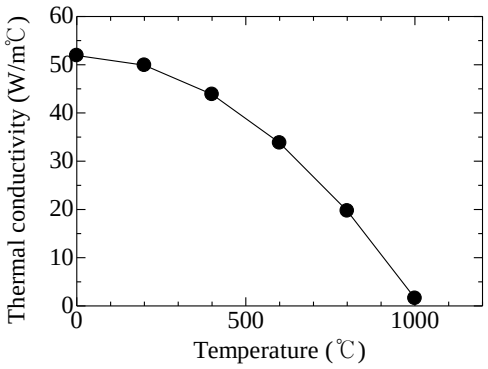

Fig. 14 Thermal conductivity (steel)

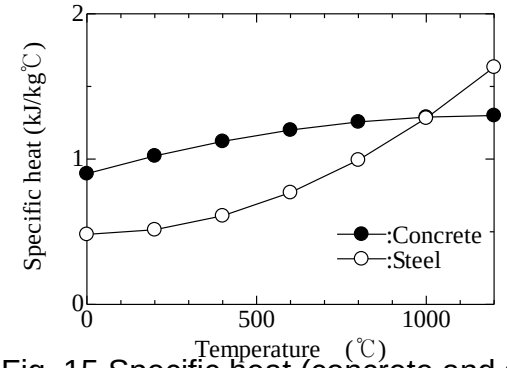

Fig. 15 Specific heat (concrete and steel)

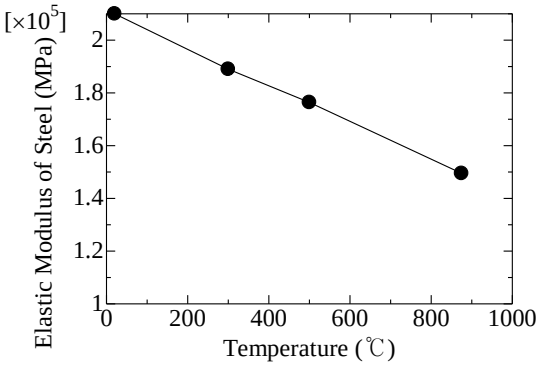

Fig. 16 Residual elastic modulus of steel

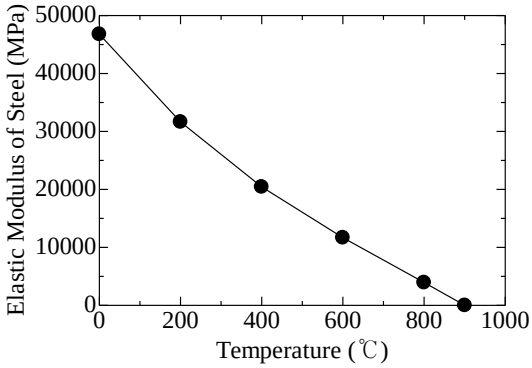

Fig. 17 Residual elastic modulus of concrete

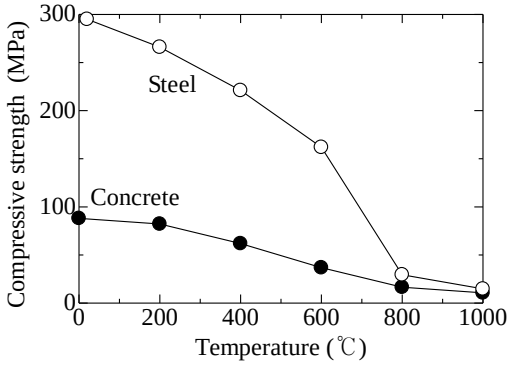

Fig. 18 Residual compressive strength (concrete and steel)

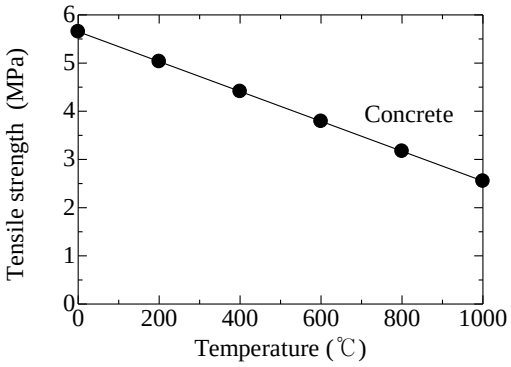

Fig. 19 Residual tensile strength of concrete

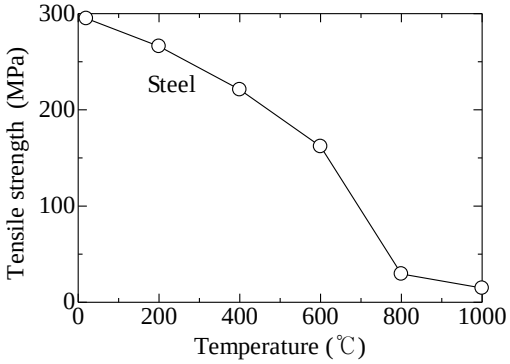

Fig. 20 Residual tensile strength of steel

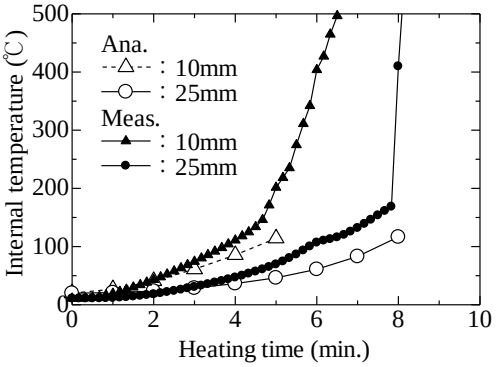

Fig. 21 Internal temperature (Meas. vs. Ana.)

4.3 Results and discussion

Figure 21 shows temperatures during heating as determined from analysis. The values at 10 and 25 mm are similar to the measured temperatures. The measurement values at 10 mm exhibit a significant change at 5 minutes, when spalling was observed. The temperature determined from analysis at 25 mm was similar to the measured value. Figure 22 shows a comparison of experimental and analytical spalling depths. It can be seen that the maximum estimated value was around 50 mm at 12 minutes. These outcomes clearly indicate that the proposed model can be used to analyze spalling depth up to 12 minutes from the start of heating. In this study, the application of 500 μ as the ultimate strain upon tensile failure produced favorable results in spalling depth calculation up to 12 min.

Figure 23 shows temperature development contour representation and spalling depth at 3, 8 and 12 min. No spalling had occurred after 3 min. of heating, but was observed at 8 and 12 min. with depths of 25 and 50 mm, respectively.

These outcomes clearly demonstrate the effectiveness of the proposed model, especially for spalling depth estimation up to 12 min.

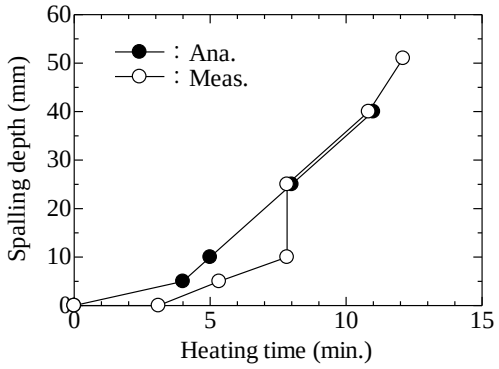

Fig. 22 Spalling depth and time (Meas. Vs. Ana.)

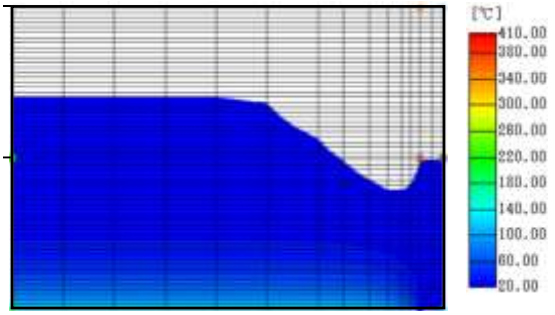

Fig. 23 a) Temperature contour and spalling after 3 min of heating

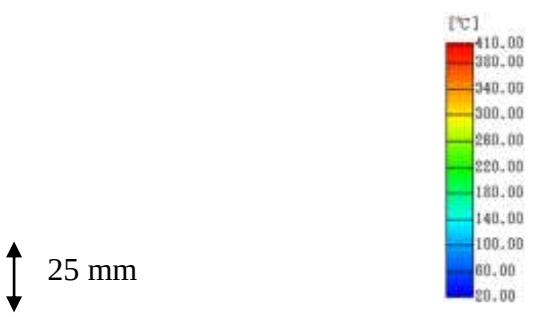

Fig. 23 b) Temperature contour and spalling depth after 8 min. of heating

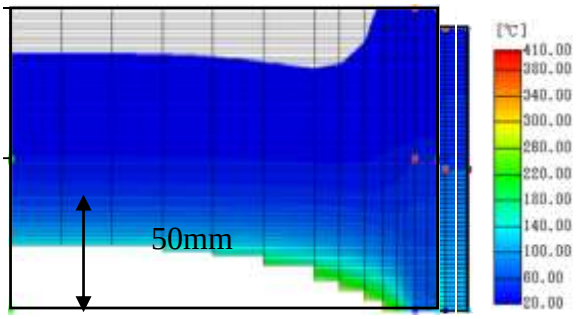

Fig. 23 c) Temperature contour and spalling depth after 12 min. of heating

5. CONCLUSIONS

In this study, numerical analysis of explosive spalling in high-strength concrete exposed to high-temperature conditions was performed in ring restraint testing using an axial symmetry model with the finite element method.
The following conclusions were drawn:

1) Analysis temperatures were similar to measured temperatures.
2) The maximum estimated spalling depth was around 50 mm at 12 minutes. The results indicate that the proposed model can be used to analyze spalling depth up to 12 minutes from the start of heating.
3) Adoption of a value of 500 μ for the ultimate strain upon tensile failure produced favorable results for spalling depth calculation up to 12 min.
4) The experimental outcomes clearly show the viability of the proposed model, especially for spalling depth estimation up to 12 min.

In future work, a spalling model allowing consideration of vapor pressure and heat from concrete-related vaporization will be developed.

Acknowledgement

This study was financially supported by the East Nippon Expressway Company Limited (NEXCO East) and by a Grant-in Aid for Scientific Research C (General) from the Japan Society for the Promotion of Science (No. 25420459; head: Dr. M. Ozawa).
The authors would like to express their gratitude to these organizations for their financial support.

REFERENCES

Ulm F. J. et al. (1999), “The Chunnel Fire. II Analysis of concrete damage,” Journal of Engineering Mechanics. 125, 283-289
Anderberg Y.(1997), “Spalling phenomena in HPC and OC,” Proceedings of the

International Workshop on Fire Performance of High-Strength Concrete, Phan, L. T., Carino, N. J., Duthinh, D., Garboczi, E. (eds.), Gaithersburg, MD: NIST, 69-73

Kalifa P. et al. (2000), “Spalling and pore pressure in HPC at high temperatures,” Cement and Concrete Research, 30,1915-1927

Phan L. T.(2000), “Pore pressure and explosive spalling in concrete,” Materials and Structures, 41, 1623-1632

Tanibe.T. et al.(2014), “Steel Ring-based Restraint of HSC Explosive Spalling in High-temperature Environments,” Journal of Structural Fire Engineering, Volume 5, Number 3, 239-250

Timoshenko S. et al.(1959), “Theory of Plates and Shells,” second edition, McGraw-Hill Book Company

C. E. Majorana et al.(2010), “An approach for modelling concrete spalling in finite strains,” Mathematics and Computers in Simulation 80,1694–1712

Michel B. et al. (2015), “Hygro-thermo-mechanical analysis of spalling in concrete walls at high temperatures as a moving boundary problem,” International Journal of Heat Mass transfer 85,110-134